Origin of Hydrocarbons Stability from a Computational Perspective: A Case Study of Ortho-Xylene Isomers

Mariusz P. Mitoraj,*[a] Filip Sagan,[a] Dariusz W. Szczepanik,[a] Jurgens H.de Lange,[b] Aleksandra L. Ptaszek,[a] Daniel M. E. van Niekerk,[b] and Ignacy Cukrowski*[b]

[a] Department of Theoretical Chemistry Faculty of Chemistry, Jagiellonian University in Krakow Gronostajowa 2, 30-87 Krakow, Poland E-mail: mitoraj@chemia.uj.ed

[b]Department of Chemistry Faculty of Natural and Agricultural Sciences University of Pretoria, Lynnwood Road, Hatfield, Pretoria 0002, South Africa E-mail: ignacy.cukrowski@up.ac.za

Abstract

It is shown herein that intuitive and text-book steric-clash based interpretation of the higher energy "*in-in*" xylene isomer (as arising solely from the repulsive CH···HC contact) with respect to the corresponding global-minimum "*out-out*" configuration (where the clashing C−H bonds are tilted out) is misleading. It is demonstrated that the two hydrogen atoms engaged in the CH···HC contact in "*in-in*" are involved in attractive interaction so they cannot explain the lower stability of this isomer. We have proven, based on the arsenal of modern bonding descriptors (EDDB, HOMA, NICS, FALDI, ETS-NOCV, DAFH, FAMSEC, IQA), that in order to understand the relative stability of "*in-in*" versus "*out-out*" xylenes isomers one must consider the changes in the electronic structure encompassing the entire molecules as arising from the cooperative action of hyperconjugation, aromaticity and unintuitive London dispersion plus charge delocalization based intra-molecular CH···HC interactions.

Keywords: aromaticity; homopolar dihydrogen bonding; hydrocarbons stability; hyperconjugation, London dispersion forces

1 Introduction

Chemistry dates back to the B.C. period and therefore it has developed primarily upon empirical observations.[1] Such observations have allowed to establish a number of useful chemical concepts, which helped interpreting and rationalizing the observed phenomena.[1] One of the best examples is the concept of steric hindrance – according to the IUPAC terminology it "arises from crowding of substituents".[2] It is, for instance, well recognized and intuitively understandable that the eclipsed ethane conformer (containing aligned C−H bonds) is less stable than the corresponding staggered configuration. Classically, it has been interpreted as originating solely from the superior steric C−H/C−H repulsion in the former case.[3] A while later a hyperconjugation effect has been identified as a cofactor determining the superior stability of staggered vs. eclipsed ethane.[3] The VSEPR theory[4] is another well recognized and useful example in which the overall repulsion between lone electron pairs is a priori assumed. However, it is now understood that some atoms surrounded by electron pairs might exhibit an electron deficient regions (so called σ/π-holes), what leads to attractive interactions with nucleophiles.[5] Another illustration is the aromaticity term originally introduced just to distinguish different odours of unsaturated homologues as compared to

typical saturated hydrocarbons – nowadays, a number of quantum chemistry based aromaticity criteria exists.[6] In spite of the substantial progress in this field, transition metal based systems still constitute a real challenge for most of aromaticity quantifiers.[7] These examples clearly demonstrate that intuitively correct concepts and interpretations established before the quantum chemistry was born, though in many cases correctly capture some parts of the reality, often lack some crucial physical contributions. To this end, they still must be deeply explored (both computationally and experimentally), verified and further developed.

In the same vein, Wagner and Schreiner[8] as well as Liptrot and Power,[9] in their comprehensive reviews have nicely tried to redefine borders between the orthodox steric repulsion concept and dispersive stabilization in sterically demanding organic and organometallic systems. It is now clear that bulky substituents add significant dispersion stabilization, which in many cases can compensate over the Pauli (kinetic) repulsion.[8, 9] As selected examples: Bistoni and co-workers have performed a series of accurate CCSD(T) calculations for various chemical bonds in bulky species and discovered the importance of London dispersion energy,[10] we have recognized stabilizing role of inter-molecular CH···HC dihydrogen interactions in organic and metaloorganic polimeric structures[11] similarly to Datta et al.,[12] Krapp et al.,[12b] Escheveria et al.,[13] and Shaik et al.[14] in a series of other sizeable species.

An intriguing and of general importance a fundamental question arises at this point – namely, are intra-molecular CH···HC dihydrogen interactions attractive in relatively small organic molecules? It has been recently demonstrated,[15a, 22] using various bonding descriptors, that the lower stability of the *cis*-2-buthene vs. *trans*-2-buthene is rooted in the destabilization of the 'bottom' ethylenic CH=CH fragment, contrary to the classical intuitive interpretation based on the 'top' CH···HC steric-repulsion.[15c, 15d] Remarkably, we have also discovered the CH···HC stabilization in *trans*-2-butene,[15a] which is formed between C−H bonds of the methyl and ethylenic units. It is also important to reference the pioneering and controversial discussions on CH···HC contacts in biphenyl.[15d–15j] These results prove that the origin of hydrocarbons stability, as well as the nature of intramolecular CH···HC interactions, is not straightforwardly predictable and, accordingly, it must be further deeply studied by various methods of quantum chemistry. Equally important is that one should not focus solely on an arbitrarily (and intuitively) selected region of a molecule when rationalizing relative stability of its isomers – therefore, very careful and open-minded approach is warranted when intuitively applying concepts that are deeply rooted in chemistry. Even more crucial for chemistry is to confront these old concepts with modern wavefunction-based methods.

Accordingly, in our further quest of comprehensive work toward in depth understanding of hydrocarbons stability, this contribution aims at shedding light on the origin of relative energies between the two xylene isomers (labelled as *out-out* and *in-in*) in terms of well recognized concepts in chemistry, Figure 1. These conformers contain the methyl units located at ortho-position – the lowest ground state isomer is characterized by the C−H bonds which are tilted out of each other (hence the label *out-out*), whereas the higher energy *in-in* structure contains the clashing CH···HC interaction, Figure 1. Additionally, the intermediate-isomer *in-out* will be considered for a brief comparison. This is a case study to describe, verify and pinpoint a possible interplay between well-recognized chemical concepts starting from the typical textbook steric-repulsion, going through hyperconjugation electronic effects to end up with the aromaticity (resonance) phenomena. To this end, our main goal herein is to shed novel light on the origin of relative stability of xylene isomers due to applying a wide spectrum of chemical bonding and electronic structure descriptors starting from the electron

density of delocalized bonds EDDB method[7c, 16] suitable for qualitative and quantitative investigations of electron delocalization and aromaticity (additionally to the HOMA and NICS tools) and the recently proposed FALDI-based conformational deformation density,[17] going through the MO based charge and energy decomposition scheme ETS-NOCV,[18] DAFH eigenvectors,[19] to end up with the real-space based QTAIM,[20] Interacting Quantum Atoms (IQA)[21] and FAMSEC[22] approaches. Their main ideas are in brief described in Experimental Section, whereas more details can be found in the ESI file (separately as parts 1–4).

Method	ΔE (kcal/mol)		
	out-out	in-out	in-in
DFT/BLYP-D3(BJ)/TZ2P	+0.00	+1.28	+2.60
DFT/BP86-D3(BJ)/TZ2P	+0.00	+1.20	+2.51
DFT/PBE-D3(BJ)/TZ2P	+0.00	+1.23	+2.56
DFT/B3LYP-D3(BJ)/TZ2P	+0.00	+1.21	+2.65
DFT/PBE0-D3(BJ)/TZ2P	+0.00	+1.14	+2.62
MP2/cc-pVTZ	+0.00	+1.56	+2.81
CCSD/cc-pVTZ	+0.00	+1.20	+2.71

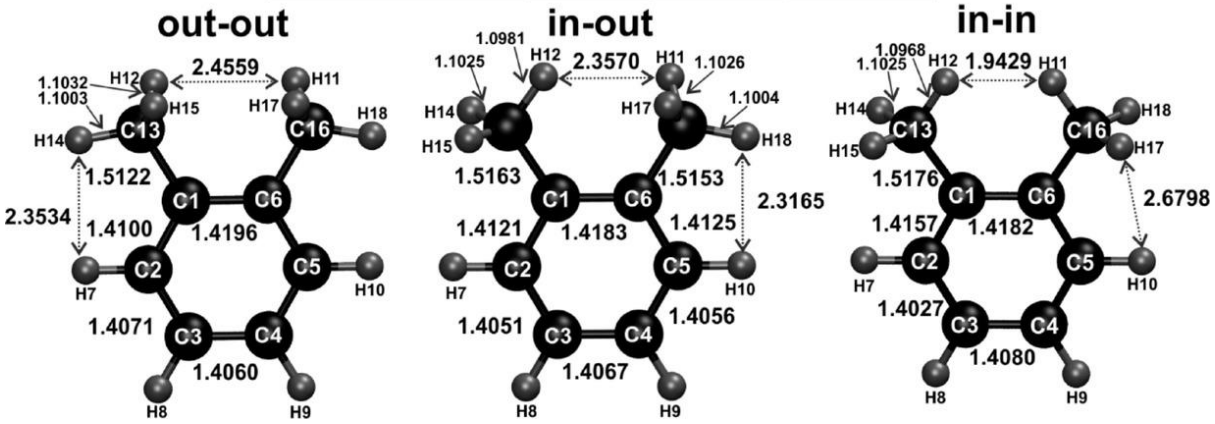

Figure 1. Relative energies based on DFT and wavefunction methods together with the selected bond lengths and interatomic distances (in Å) in *out-out* (global minimum), *in-out* (TS- first order saddle point) and *in-in* (local minimum) conformers of xylene.

2 Results and Discussion

An analysis of the stability of three o-xylene isomers with the use of an array of methods, including the DFT, MP2 and CCSD, provided their relative energies, as presented in Figure 1. The global minimum *out-out* isomer is consistently more stable by 2.5–2.8 kcal/mol than *in-in* isomer (also minimum energy structure) and by 1.1–1.6 kcal/mol with respect to the transition state *in-out* regardless of the method applied, Figure 1. It is in accord with the theoretical (low level HF) investigations.[23] The experimentally determined methyl rotor barriers which range (depending on a technique applied) between ~500–700 cm^{-1} (1.4–2.0 kcal/mol)[23c] also fit well to our estimations, Figure 1.

Let us at first stage describe the interaction between Me units and phenyl rings – in order to achieve this goal we have applied our charge and energy decomposition method ETS-NOCV which enables to extract and quantify various bonding constituents (σ, π, δ, etc.).[18] The obtained results demonstrate, interestingly in line with the stability order of *o*-isomers, that the methyl unit in *out-out* is the strongest bonded to the phenyl ring with respect to both remaining conformations: *in-in* (by ca. ΔE_{int}~2 kcal/mol) and *in-out* (by ca. ΔE_{int}~0.8 kcal/mol), Figure 2, Figure 1. It correlates very well with the systematic elongation of the C−C distances from 1.5122 Å for *out-out* going through 1.5163/1.5153 Å for *in-out* to end up with 1.5176 Å in the case of *in-in*, Figure 1. Since the structural and energetic differences

between *out-out* and clearly the intermediate *in-out* are very minute, in the forthcoming sections we shall focus predominantly on comparison between *out-out* vs. *in-in* (both minima) for which the obtained differences are the most pronounced (and accordingly they are quantitatively discussible).

Interestingly, although the methyl unit in *out-out* experiences slightly more Pauli (kinetic) repulsion [due to σ(C−H)/π(C=C) overlaps] by ca. 1.30 kcal/mol as compared to *in-in*, it is easily overcompensated by more pronounced charge delocalization [ΔE_{orb} by 1.2 kcal/mol] and electrostatic [ΔE_{elstat} by 1.7 kcal/mol] terms giving rise to the overall interaction energy ΔE_{int}=−117.7 kcal/mol for *out-out* and ΔE_{int}=−115.9 kcal/mol for *in-in*, Figure 2A. The ETS-NOCV estimated methyl bonding constituents for *in-out* (and *out-in*) falls roughly in between *out-out* and *in-in*, Figure 2A.

In order to further understand the origin of more pronounced ΔE_{orb} for *out-out* vs. *in-in* we have decomposed the corresponding $\Delta\rho_{orb}$ into the NOCV's based contributions $\Delta\rho_{orb}$(i), Figure 2B. The major channel $\Delta\rho_{orb}(\sigma)$ clearly shows formation of the covalent C−C bond between the methyl and phenyl ring what corresponds to $\Delta E_{orb}(\sigma)$=−179.9 kcal/mol for *out-out* and it is slightly more stabilizing than the corresponding $\Delta E_{orb}(\sigma)$=−178.6 kcal/mol for *in-in*, Figure 2B. Importantly, we have also extracted the π-type deformation density channel, perpendicular to the phenyl ring, $\Delta\rho_{orb}(\pi)$ showing the hyperconjugation-type effects which originate from the intra-methyl σ(C−H)→σ*(C−H) and intra-phenyl π(C=C)→π*(C=C) charge delocalizations, Figure 2B. It can be considered as a response of π-electron density to Pauli repulsion which is in turn induced by efficient σ(C−H)/π(C=C) overlaps. Such π-delocalization (aromaticity) is more pronounced for *out-out* vs. *in-in*, Figure 2B. The former σ(C−H)→σ*(C−H) charge delocalization is consistently reflected in a slight elongation of the engaged C−H bonds by ∼0.001 Å upon *in-in* → *out-out* transition Figure 1. Non-equivalence of the in-plane (H_{in}) and out-of-plane (H_{out}) methyl C−H bonds is also seen from the experimental gas-phase overtone spectra[23d] and from our calculated C−H frequencies (ESI, part 2, Table 2.2 and Figure 2.11).

It shall be pointed out, that the above ETS-NOCV results demonstrating more efficient π-resonance (at phenyl ring) as well as within the methyl units in *out-out* vs. *in-in* have been confirmed by the aromaticity calculations by means of the three well recognized descriptors: representing structural-based (HOMA),[7a] magnetic- (NICS),[7b] and the electronic based (EDDB),[7c, 16] ESI, part 3, Table 3.1. We have determined that both resonance delocalizations are more pronounced in the case of *out-out* (by ∼2.7 % at Me units and by ∼7 % at Ph ring). These results demonstrate that the presence of four C−H bonds (within the two Me units) interacting between each other and with the phenyl ring in *out-out* with respect to only two clashing C−H bonds in *in-in*, results not only in a more pronounced methyl binding energy (reflected by the shortening of the corresponding C−C(Me) bonds), but also in amplification of the π-electron density changes (resonance) at the phenyl ring. The latter is in turn reflected by an increase of the aromaticity for *out-out* vs. *in-in* (ESI, part 3, Table 3.1).

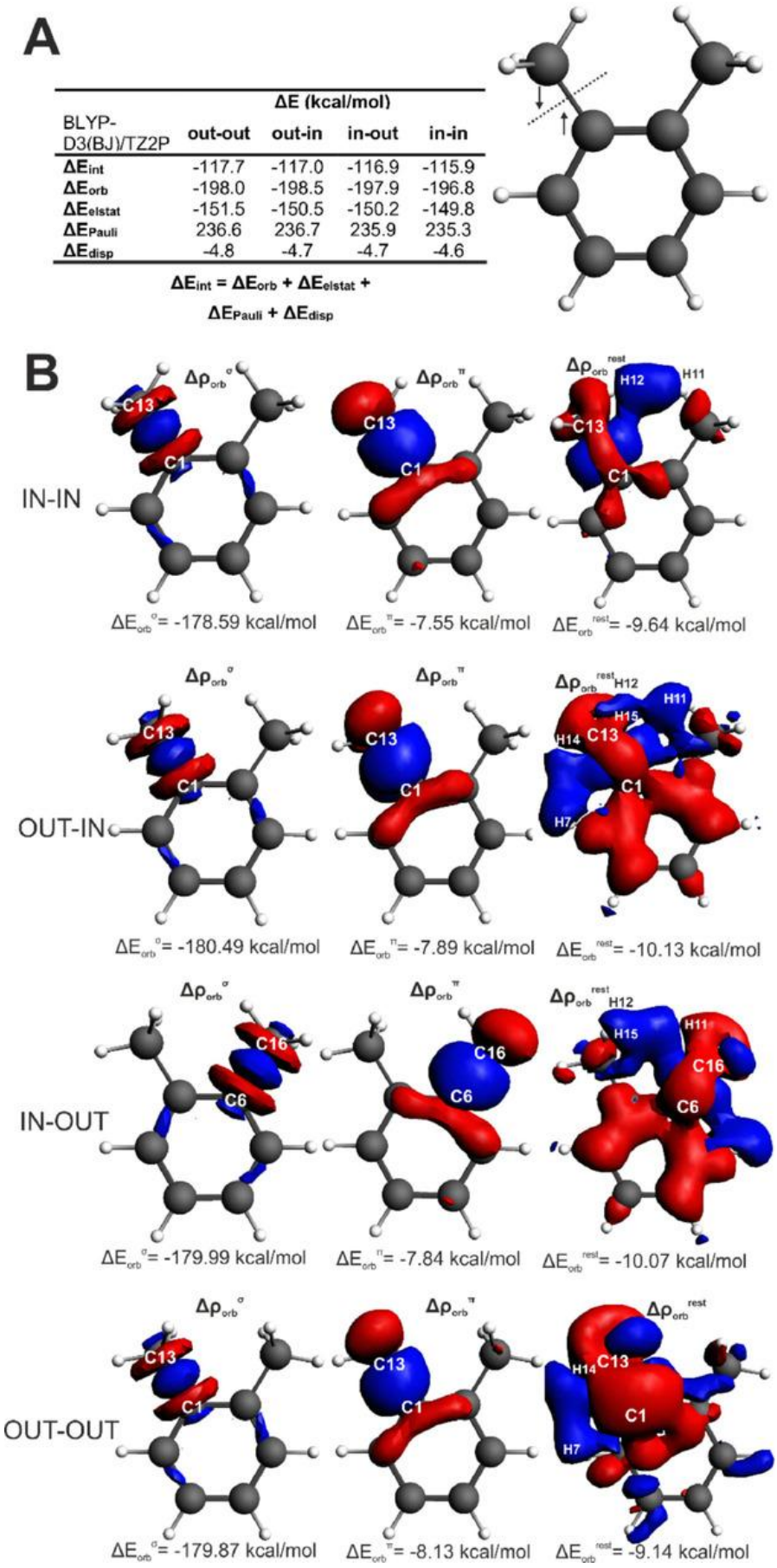

Figure 2. ETS-NOCV results describing the methyl bonding in *out-out* vs. out-in, *in-out* and *in-in*.

It is finally crucial to point out that, apart from the already determined major effects, one can additionally notice formation of the secondary weak charge delocalizations due to the bay-type CH11···12HC contacts in *in-in* isomer $\Delta\rho_{orb}$(rest) and astonishingly the side-type CH14···7HC/ CH18···10HC (see Figure 2B) as well as the bay-type CH12···11HC/{CH17···15HC interactions in *out-out* conformation, (ESI, part 2, Figure 2.6). The latter silent interactions discovered in *out-out* are observed despite the fact, that they lack corresponding QTAIM bond critical points as opposed to the one detected only for CH11···12HC in *in-in*. It shall be pointed out that the charge density accumulation between the corresponding hydrogen atoms [*in-in*: H11···H12, *out-out*: H14···H7/H18···10H, H12···H11, H17···H15] is also visible when considering the overall deformation density $\Delta\rho_{total}$ plots (ESI, part 2, Figures 2.6–2.7) and DAFH eigenvectors (ESI, part 2, Figure 2.8), what proves that the Pauli doesn't fully cancel out the 'electronic' stabilization. Our conclusions are valid regardless of the fragmentations applied (ESI, part 2, Figure 2.6, Figure 2.7). Similar conclusions are valid when considering the conformational deformation density descriptor (ESI part 4, Figure 4.1). Detailed analyses of (3,−1) CP(H12,H11) in *in-in* and its close vicinity indicate, that the entire C13−H12/C16−H11 fragments participate in the bonding, therefore, it is more appropriate to refer to this interaction as C13H12···H11 C16 rather than H12···H11 (ESI part 4, Figure 4.5, Table 4.2).

To further support these findings we have performed ^{1}H NMR calculations for *out-out* and *in-in* – the results gathered in ESI (part 2, Figure 2.9) nicely differentiate the hydrogen atoms involved in the mentioned dihydrogen (bay and side-types) interactions. Since the NOCV deformation density channels corresponding to the identified dihydrogen contacts are significantly delocalized and it is impossible to quantify (through ETS-NOCV) their all constituents, in the forthcoming sections we have decided to make use of simply atomic energies as well as the recently developed IQA[21]-based FAMSEC[22] (real space fragment attributed molecular system energy change) approach which allows to analyse the nature of chemical bonding in the atomic resolution. It will be also expressed and discussed in terms of interactions between larger molecular fragments. Details of FAMSEC are found in ESI (part 1).

It is reasonable to assume that the energy of atoms involved in a steric clash destabilising the *in-in* conformer should increase as, according to classical interpretations, they should become strained. A topology of $\Delta E_{\mathrm{add}}^{\mathrm{A}}$ distribution throughout a molecule (it was computed on the *out-out*→*in-in* transformation) is shown in Figure 3a (a full set of data is included in the ESI, part 1, Figure 1.1, Table 1.1). For clarity, only atoms for which $\Delta E_{\mathrm{add}}^{\mathrm{A}}$ >±0.05 kcal/mol are marked. It is important to recall that these atomic energies are additive meaning that the sum of changes in the $\Delta E_{\mathrm{add}}^{\mathrm{A}}$ values is equal to the change in electronic energies of the two conformers, $\Delta E=E_{in\text{-}in}-E_{out\text{-}out}$. There are only four atoms (two atom-pairs) that experienced a decrease in their energies and each atom of the 'clashing' H11−H12 atom-pair became stabilised most and 5-times more that the C1/C6 atom-pair of the ring.

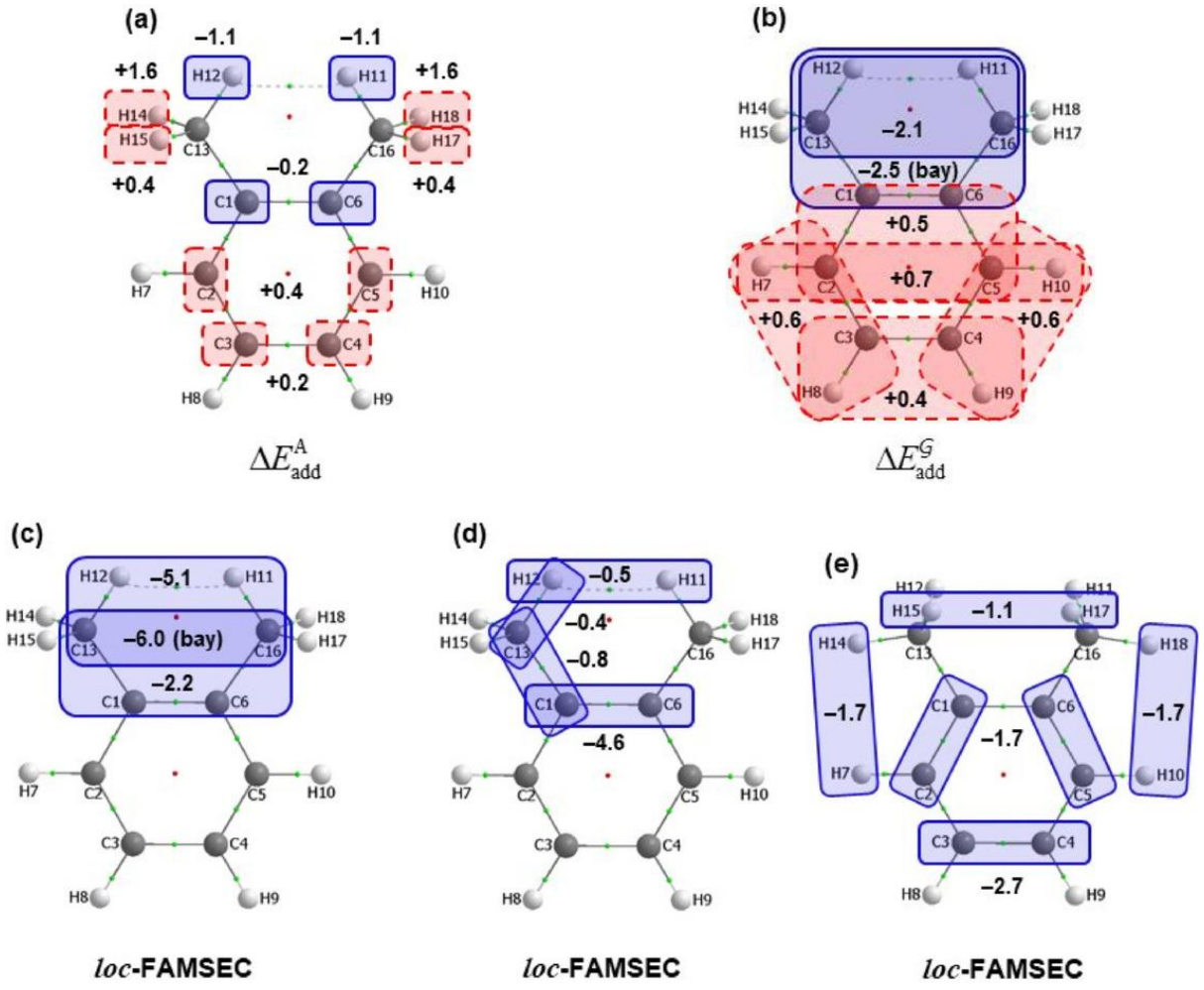

Figure 3. Topology of changes in additive atomic (part a) and fragment's energies (part b) as well as selected *loc*-FAMSEC energy terms computed for the indicated molecular fragments on the *out-out→in-in* (parts c and d) and *in-in→out-out* (part e) structural changes of xylene. Atoms and fragments stabilized are marked by blue coloured solid-line rectangles and destabilised by red coloured dashed-line rectangles. All values are in kcal/mol.

Furthermore, by summing up additive energies of atoms of the CH11···H12 C fragment and the bay, we obtained −2.1 and −2.5 kcal/mol, respectively, showing that these fragments' additive energies decreased. Hence, neither the H11···H12 and CH11···H12 C fragments nor the bay can be linked with $\Delta E = E_{in\text{-}in} - E_{out\text{-}out}$ =+2.8 kcal/mol computed at the MP2 level. Notably, among atoms that became destabilised, H14 and H18 experienced most significant increase in energy (ΔE^{A}_{add} =+1.6 kcal/mol) that is four times larger than the second in value +0.4 kcal/mol obtained for the H15/H17 and C2/C5 atom-pairs. This means that on the *in-in→out-out* change the H14/H18 would become most stabilised (with ΔE^{A}_{add} =−1.6 kcal/mol each) whereas H11/H12 most destabilised (with ΔE^{A}_{add} =+1.1 kcal/mol each). This clearly demonstrates that the homopolar CH···HC dihydrogen interactions involving CH7/CH10 of phenyl and the CH14/CH18 of methyl groups in *out-out* (i. e., the "side" CH7···H14 C and CH10···H18 C interactions) as well as CH11/CH12 of both methyl groups in the *in-in* conformer lead to the decrease of relevant H-atoms' energies, hence also decrease the electronic energies of respective xylene conformers.

We have also performed a similar analysis for the *out-out*→*in-out* transformation (ESI, part 1, Table 1.1). Data obtained shows that the rotation of a single Me functional group (−C13H$_3$) resulted in a decrease of the additive energy of H12 by very much the same value of −1.1 kcal/mol as found for the *out-out*→*in-in* transformation even though H12 is not involved is steric clashes with H11 and H17 due to the interatomic distances of 2.36 Å. This finding conclusively shows that the stabilising in nature change in the $\Delta E_{\rm add}^{\rm A}$ values computed for H12/H11 on either single or double Me functional group rotation has nothing to do with relative position of these two atoms. Further support is provided by the data in the ESI (part 1, Table 1.1) that shows that step-wise Me groups rotations, from *out-out* to *in-out* followed by *in-out* to *in-in* (where H12 and H11 are in steric contact) resulted in the decrease in additive atomic energies of H12 and H11 by the same value of −1.1 kcal/mol. Also, a simultaneous rotation of both Me groups produced the same output in terms of these H-atoms additive energy change. These findings are in direct contrast to classical thinking on one hand and on the other clearly suggest that there must be other reason of the observed phenomenon.

An additional insight can be gained from the analysis of the *loc*-FAMSEC terms that quantify energy changes entirely restricted to the 3D space occupied by a selected molecular fragment. With focus on the bay where H12 and H11 are involved in a steric contact (Figure 3c) we found that on *out-out*→*in-in* the C13H12···H11 C16 and C13-C1-C6-C16 fragments have been stabilised by −5.1 and −2.2 kcal/mol, respectively. As a matter of fact the entire bay has been stabilised significantly (by −6.0 kcal/mol) and, from the 2-atom perspective, the H12–H11 contact in *in-in* experienced a small decrease (by −0.5 kcal/mol – Figure 3d) in the energy confined to the 3D space occupied by the two atoms. These data corroborate with changes in additive energies, either atomic or that of a fragment, very well and provide additional and quantified argument against destabilising impact of the steric H12–H11 contact in the *in-in* higher energy isomer of xylene (note that all bonded atom-pairs of the bay became locally stabilised and among them the C1−C6 fragment experienced most negative *loc*-FAMSEC of −4.6 kcal/mol; Figure 3d). Finally, selected relevant fragments that became stabilised on the opposite structural change, *in-in*→*out-out*, are shown in Figure 3e – the most crucial is gain of the "side" H7···H14/H10···H18 stabilisation as well as the "bay" type from H15···H17 which fully corroborates the results from ETS-NOCV and other approaches (FALDI, DAFH, ESI, parts 2 and 4). A large set of *loc*-FAMSEC data computed for numerous molecular fragments is included and discussed in part 1 of the ESI.

All the above data provides undeniable multiple evidence that the classical interpretation of xylene *in-in* conformer's instability (with respect to *out-out*) is entirely wrong. It is absolutely clear that not only the 'steric' H11–H12 contact in the *in-in* conformer must be seen as a H11···H12 interaction of stabilising nature ($E_{\rm int}^{\rm H11,H12}$ =−4.8 kcal/mol) but the battery of different descriptors revealed that on *out-out*→*in-in* these two atoms experienced stabilising in nature $E_{\rm int}^{\rm H11,H12}$ of −3.5 kcal/mol that is most significant among all 153 atom-pairs, they became most stabilised in terms of their atomic additive energies ($\Delta E_{\rm add}^{\rm A}$ =−1.1 kcal/mol), the entire 3D space occupied by them experienced energy change in a stabilizing manner (*loc*-FAMSEC<0), and they found themselves in most friendly molecular environment with most significant change in $\Delta E_{\rm int}^{\rm A,R}$ of −5.2 kcal/mol. The latter energy term quantifies the interaction energy change between an atom A and all the remaining atoms of a molecular system treated as a fragment R. It is a useful energy term as it can be attributed to how 'friendly' (or otherwise) a new molecular environment became toward a selected atom and, e. g., $\Delta E_{\rm int}^{\rm A,R}$ <0 points at attractive in nature change in interactions between A and R. A final nail to the coffin of classical interpretation of the H−H contacts comes from the *mol*-

FAMSEC term (Figure 4) that describes an energy contribution of a selected molecular fragment to the molecular system on this system change from any *initial* to a *final* state/structure. The H11/H12 molecular fragment has made an energy contribution of stabilizing nature to the *in-in* conformer with *mol*-FAMSEC=−3.8 kcal/mol (Figure 4a) and this is the largest (most negative) contribution made among all unique (153) 2-atom fragments. It must be finally noticed, in line with the above observations, that at present time intra-molecular CH···HC in planar biphenyl are also found attractive in the recent works based on the powerful methods IQA,[15e] FAMSEC,[22] IQA/REG[15i] and pioneering QTAIM[15g, 15h] as opposed to the repulsive text-book interpretation favoured till now only in Ref [15d].

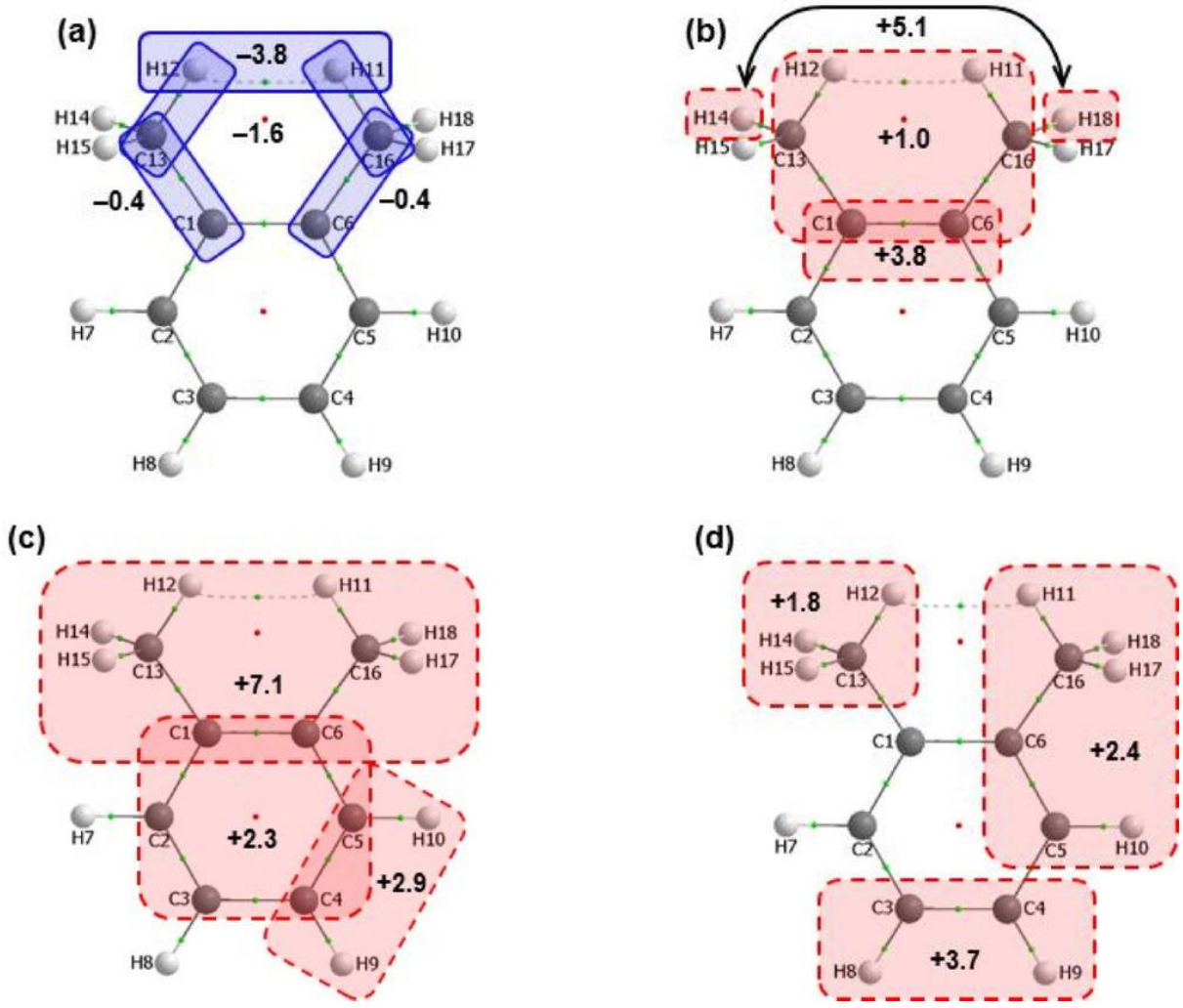

Figure 4. Topology of *mol*-FAMSEC energy terms computed for the indicated molecular fragments on the *out-out*→*in-in* structural change of xylene. Fragments marked by blue-coloured solid-line rectangles and red-coloured dashed-line rectangles made significant contribution to molecular stability and instability, respectively. All values are in kcal/mol.

Hence, why *in-in* is the higher energy conformer of xylene? Figure 4 shows that the relative stability of the conformers cannot be attributed to a single molecular fragment and this is consistent with a picture recovered from analysis of atomic and fragment additive energies as well as *loc*-FAMSEC terms discussed above. To this effect and following classical approach in terms of paying attention just to two atoms, H14/H18 made largest positive contribution (*mol*-FAMSEC=+5.1 kcal/mol, Figure 4b); hence, they destabilised *in-in* most among 153 2-atom fragments of xylene. Notably, this correlates very well with these atoms most signify-

cant increase in additive atomic energies (Figure 3a). Moreover, C1/C6 is the only 2-atom fragment of the bay that destabilised *in-in*. We are of an opinion that it makes perfect sense to consider meaningful larger fragments (i. e. MeC=CMe) – clearly less efficient hyperconjugation effects and consequently weaker methyl binding energies (as indicated by ETS-NOCV data) results in the enormous destabilisation of the entire top MeC=CMe of *in-in* isomer as revealed by *mol*-FAMSEC=+7.1 kcal/mol (Figure 4c). The entire bottom aromatic ring of *in-in* is also destabilized to lesser extend with *mol*-FAMSEC=+2.3 kcal/mol, Figure 4c, which is in perfect accordance with the relatively weaker aromatic character (ESI, part 3). The "top" bay itself also made unfavourable contribution but much smaller (*mol*-FAMSEC=+1.0 kcal/mol) and clearly this is mainly due to contributions made by C1/C6 and not H11/H12 that made contribution of stabilising nature. Methyl functional groups made relatively small unfavourable contribution (*mol*-FAMSEC=+1.8 kcal/mol, Figure 4d) only because they contain H11/H12 atoms that largely compensated highly positive contribution made by H14/H18. Clearly, regardless how one selects molecular fragments, our analysis demonstrates important roles played by H11/H12 and H14/H18 atom-pairs that, respectively, stabilised and destabilised *in-in* relative to *out-out* most. For those interested, a large set of *mol*-FAMSEC data is included in part 1 of the ESI. Finally, it is customary to reference, that London dispersion forces is a crucial component of intramolecular dihydrogen bonding C−H···H−C in addition to charge delocalization contribution.[15a] The importance of the latter term in other untypical anion-π interactions has been also recognized.[26] To further reference, an excellent review on homopolar dihydrogen contacts in hydrogen storage materials is available in Ref. [27]. Furthermore, Myburgh and co-workers have also found, in line with our observations herein, a negative exchange-correlation term for the sterically congested H−H atoms in cyclic hydrocarbons.[15l] Proton NMR chemical shifts have appeared to loosely correlate with the exchange-interaction energies for the considered cyclic hydrocarbons.[15m] Although, the nature of close C−H···H−C contacts is still controversial,[29] it shall be noticed, that more and more suggestions appear in the recent literature which highlight the importance of rather attractive C−H···H−C contacts.[15a, 15b, 15e, 15i, 22, 30-33]

3 Conclusions

This work provides in-depth physical understanding of higher stability of the global minimum *out-out* xylene isomer (where four methyl C−H bonds are titled out of the phenyl ring) with respect to the corresponding *in-in* rotamer (containing close C−H···H−C contact) based on the arsenal of quantum chemical methods and bonding descriptors starting from electron delocalization (EDDB) and aromaticity (HOMA, NICS) descriptors, going through FALDI-based conformational deformation density, molecular orbitals based the charge and energy decomposition scheme ETS-NOCV to end up with the real-space based: QTAIM and FAMSEC scheme rooted in the Interacting Quantum Atoms (IQA) energy decomposition. Even though such unprecedented large diversity of different quantum chemical methods was used, a remarkable agreement among numerous fundamental properties is observed that, in our opinion, strongly supports our interpretation and major conclusions. First of all, contrary to the text-book and literature[23c] intuitive steric-based interpretation, the two hydrogen atoms (H12···H11) engaged in the homopolar close C−H···H−C contact in *in-in* are involved in attractive interaction so they can't explain the lower stability of this isomer with respect to *out-out*. It is proven, that superior stability of *out-out* vs. *in-in* can only be understood when considering cooperative changes in the electronic structure at both the upper (MeC=CMe unit) and bottom (phenyl rings) parts of the xylene isomers. It is consistently demonstrated that *out-out* experiences more efficient, Pauli repulsion driven, intra-methyl hyperconjugation σ(C−H)→σ*(C−H) phenomenon amplifying the strength of methyl bonding and

consequently the superior stability of the entire upper bay MeC=CMe fragment as well as enhanced intra-phenyl π(C=C)→π*(C=C) resonance (aromatic) effects. Both these inter-related factors predominantly give rise to the superior stability of *out-out* vs. *in-in*. Additionally and surprisingly, the side type homopolar dihydrogen interactions formed by the methyl and phenyl C−H bonds (H7···H14/H18···H10) are also found to stabilize *out-out*. These non-covalent interactions together with the major hyperconjugation and resonance effects encompassing an entire xylene molecules make *out-out* isomer more stable than *in-in*, what proves, that it is of paramount importance to look holistically when rationalizing the relative stability of organic species. Our recent investigations[11, 15a] and the data reported herein prove that a simple application of well-recognized, though deeply rooted in chemistry concepts,1 which identify intuitively (and arbitrarily) a single region of a molecule as solely responsible for the overall stability is totally misleading. These results also suggest, that similar is likely to be valid for other hydrocarbons containing clashing C−H bonds.

Experimental Section

FALDI

Conformational deformation density (a change from a reference conformer, *ref*, to a final conformer, *fin*) is calculated as:[17]

$$\Delta_c\rho(\mathbf{r}) = \sum_{\mathrm{A}}^{M} \Delta_c\mathcal{L}_{\mathrm{A}}(\mathbf{r}) + \sum_{\mathrm{A}}^{M-1}\sum_{\mathrm{B}>A}^{M} \Delta_c\mathcal{D}_{\mathrm{A,B}}(\mathbf{r})$$

where:

$$\Delta_c\mathcal{L}_{\mathrm{A}}(\mathbf{r}) = {}^{fin}\mathcal{L}_{\mathrm{A}}(\mathbf{r}) - {}^{ref}\mathcal{L}_{\mathrm{A}}(\mathbf{A}_{\mathrm{A}}\mathbf{r})$$

is the change in core density at **r** for atom A calculated through $\mathbf{A}_{\mathrm{A}}$ which is a transformation matrix relating the relative position and orientation of an atom A in *fin* to its position and orientation in *ref*. The resulting change in a specific diatomic delocalized density contribution is:

$$\Delta_c\mathcal{D}_{\mathrm{A,B}}(\mathbf{r}) = {}^{fin}\mathcal{D}_{\mathrm{A,B}}(\mathbf{r}) - {}^{ref}\mathcal{D}^{\mathcal{R}}_{\mathrm{A,B}}(\mathbf{r})$$

where ${}^{ref}\mathcal{D}^{\mathcal{R}}_{\mathrm{A,B}}(\mathbf{r})$ refers to the weighted contribution of ${}^{ref}\mathcal{D}_{\mathrm{A,B}}$ at both A_Ar and A_Br.[17] More details are in the ESI file, part 4.

FAMSEC

There are two main quantities defined within FAMSEC:[22] *loc*-FAMSEC and *mol*-FAMSEC. The former is defined as:

$$loc\text{-FAMSEC} = \Delta E^{\mathrm{G}}_{\mathrm{self}} + \Delta E^{\mathrm{G}}_{\mathrm{int}}$$

where the $\Delta E^{\mathrm{G}}_{\mathrm{self}}$ term accounts for a self-fragment (G) energy change due to conformational change *ref*→*fin*. The $\Delta E^{\mathrm{G}}_{\mathrm{int}}$ term quantifies the intrafragment interaction energy change and when G is made of two atoms it quantifies a diatomic interaction energy[21] change. From this follows that *loc*-FAMSEC might be useful in identifying parts of a molecule that experienced

most significant decrease (or increase) of their energies that can be interpreted as being most stabilised (or strained, respectively) in *fin* relative to *ref*. In order to assess if G stabilizes a molecule when going to *fin* state one must account for the interaction with the remaining part of a molecule (another molecular fragment H) giving rise to *mol*-FAMSEC:

$$mol\text{-FAMSEC} = loc\text{-FAMSEC} + \Delta E_{\text{int}}^{\text{GH}}$$

More details on FAMSEC can be found in ESI, part 1.

EDDB

The EDDB(*r*) function derives from the original method of the electron density (ED) partitioning that has been introduced to provide a uniform approach to quantify electron delocalization in molecular systems ED(*r*)=EDLA(*r*)+EDLB(*r*)+EDDB(*r*), where EDLA represents electrons localized on atoms (inner shells, lone pairs), EDLB represents electrons in Lewis-like localized bonds, and EDDB represents electrons delocalized between conjugated bonds (multicenter electron sharing, aromatic rings).[7c, 16] The latter is calculated based on diatomic blocks of a charge and bond-order matrix.[7c, 16] More details are in ESI file, part 3.

DAFH

In the presented approach domain-averaged Fermi hole[19] is defined as:

$$h_\Omega(r_1) = \rho(r_1) - P_\Omega(r_1)$$

where $P_\Omega(r_1)$, subtracted from the ordinary electron density in a fixed point r_1, is the conditional probability of finding one electron of the pair in r_1, provided the second electron is allowed to move inside a certain region Ω. The universal normalization of domain-averaged Fermi hole does not depend on the choice of that region, which enables us to select holes averaged over the complex domains. The required quantity in the hole definition is the number of electrons in region Ω:

$$g_\Omega(r_1) = N_\Omega h_\Omega(r_1)$$

in which the factor N_Ω stands for a statistical correction for the actual number of electrons in Ω. Taking into consideration SCF approximation, the Eq. (3) can be rewritten in the form:

$$g_\Omega(r_1) = 2\sum_i^{occ}\sum_j^{occ}\langle i|j\rangle_\Omega \phi_i(r_1)\,\phi_j(r_1)$$

where $\{\phi_i(r_1),\ i = 1,\ldots,occ\}$, $\{\phi_j(r_1),\ j = 1,\ldots,occ\}$ are occupied orbitals and

$$\langle i|j\rangle_\Omega = \int_\Omega \phi_i(r)\,\phi_j(r)\,dr$$

presents the overlap integral over the Ω.

ETS-NOCV

The Natural Orbitals for Chemical Valence (NOCVs)[18] are eigenvectors ψ_i which constitute an unitary U matrix obtained from a simple diagonalization of the deformation density matrix ΔP^{orb} expressed in the basis of orthogonalized fragment orbitals λ_k :

$$\mathrm{U^T}\Delta P^{orb}\mathrm{U} = \mathrm{v},\ \psi_\mathrm{i} = \sum_{k=1}^{M} U_{ik}\lambda_k$$

where v is a resulting diagonal matrix collecting NOCV's eigenvalues and M stands for a number of fragment-orbitals. ΔP^{orb} (expressed in Löwdin representation) is calculated as a difference between a density matrix of a molecule and those obtained for molecular fragments. It has been shown, that NOCV's allow for decomposition of molecular deformation density $\Delta\rho_{orb}$ into chemically meaningful bonding contributions $\Delta\rho_{orb}(i)$ with different symmetries (e. g. σ, π, δ, etc.) even for molecules with no symmetry:

$$\Delta\rho_{\mathrm{orb}} = \sum_{\mathrm{i}=1}^{\mathrm{M/2}} \mathrm{v_k}(-\psi_{-\mathrm{k}}^2 + \psi_{\mathrm{k}}^2) = \sum_{\mathrm{i}=1}^{\mathrm{M/2}} \Delta\rho_{\mathrm{orb}} \quad \mathrm{(i)}$$

ETS-NOCV scheme allows for decomposition of orbital interaction term ΔE_{orb} responsible for charge delocalization due to bonding into NOCV-based contributions $\Delta E_{orb}(i)$.[18] Overall interaction energy ΔE_{total} between two fragments is divided into the following components $\Delta E_{total} = \Delta E_{dist} + \Delta E_{elstat} + \Delta E_{Pauli} + \Delta E_{orb}$. ΔE_{dist} is called distortion term and it corresponds to the energy needed for geometry change from the fragment's optimal geometry to the one in the molecule. Next term (ΔE_{elstat}) is the electrostatic interactions between fragments in their position within the molecule. The third term separates Pauli repulsion (ΔE_{Pauli}) between occupied orbitals of fragments.[18] We have applied BLYP-D3/TZP which is found to be an extremely reliable protocol for reproduction of experimental and accurate theoretical outcomes concerning the nature of non-covalent interactions[28] (ESI, part 2, Figure 2.10).

Acknowledgements

DFT calculations were partially performed using the PL-Grid Infrastructure and resources provided by the ACC Cyfronet AGH (Cracow, Poland). Ignacy Cukrowski gratefully acknowledges the National Research Foundation of South Africa (Grant Number 105855) and the Centre for High Performance Computing (CHPC), South Africa, for providing computational resources for this research project. D.W.S. acknowledges the financial support of the Polish National Science Center within the Sonata IX Project 2015/17/D/ST4/00558. Mariusz Paweł Mitoraj acknowledges the fruitful discussions with C. McKee (Georgia University) and S.A. Adjadi (Hong-Kong University) as well as the financial support of the Polish National Science Center within the Sonata Bis Project 2017/26/E/ST4/00104.

References

1 G. Frenking, S. Shaik, The Chemical Bond: Fundamental Aspects of Chemical Bonding, Wiley-VCH, Weinheim 2014.

2 A. D. McNaught, A. Wilkinson, in *IUPAC. Compendium of Chemical Terminology, 2nd ed. (the "Gold Book").*

3

3a F. M. Bickelhaupt, E. J. Baerends, *Angew. Chem. Int. Ed.* 2003, 42, 4183– 4188;

Angew. Chem. 2003, 115, 4315– 4320;

3b F. Weinhold, *Nature* 2001, 411, 539– 541;

3c F. Weinhold, *Angew. Chem. Int. Ed.* 2003, 42, 4188– 4194;

Angew. Chem. 2003, 115, 4320– 4326.

4 R. J. Gillespie, I. Hargittai, The VSEPR model of molecular geometry, Dover, NY 2012.

5

5a J. S. Murray, P. Lane, T. Clark, K. E. Riley, P. Politzer, *J. Mol. Model.* 2012, 18, 541–548;

5b P. Politzer, J. S. Murray, T. Clark, *Phys. Chem. Chem. Phys.* 2013, 15, 11178– 11189.

6

6a M. Solà, F. Feixas, J. O. C. Jiménez-Halla, E. Matito, J. Poater, *Symmetry* 2010, 2, 1156–1179;

6b F. Feixas, E. Matito, J. Poater, M. Solà, *Chem. Soc. Rev*. 2015, 44, 6434– 6451.

7

7a J. Kruszewski, T. M. Krygowski, *Tetrahedron Lett.* 1972, 13, 3839– 3842;

7b P. v R Schleyer, C. Maerker, A. Dransfeld, H. Jiao, N. J. R. van Eikema Hommes, *J. Am. Chem. Soc.* 1996, 118, 6317– 6318;

7c D. W. Szczepanik, M. Andrzejak, K. Dyduch, E. Żak, M. Makowski, G. Mazur, J. Mrozek, *Phys. Chem. Chem. Phys.* 2014, 16, 20514– 20523.

8 J. P. Wagner, P. R. Schreiner, *Angew. Chem. Int. Ed.* 2015, 54, 12274– 12296;

Angew. Chem. 2015, 127, 12446– 12471.

9 D. J. Liptrot, P. P. Power, *Nat. Rev. Chem.* 2017, 1, 0004.

10

10a G. Bistoni, A. A. Auer, F. Neese, *Chem. Eur. J.* 2017, 23, 865– 873;

10b Q. Lu, F. Neese, G. Bistoni, *Angew. Chem. Int. Ed.* 2018, 57, 4760– 4764;

Angew. Chem. 2018, 130, 4850– 4854.

11

11a M. P. Mitoraj, F. Sagan, M. G. Babashkina, A. Y. Isaev, Y. M. Chichigina, D. A. Safin, *Eur. J. Org. Chem*. 2019, 2–3, 493– 503;

11b F. Sagan, R. Filas, M. P. Mitoraj, *Crystals* 2016, 6, 28;

11c M. P. Mitoraj, M. G. Babashkina, A. Y. Isaev, Y. M. Chichigina, K. Robeyns, Y. Garcia, D. A. Safin, *Cryst. Growth Des.* 2018, 18, 5385– 5397;

11d F. Sagan, Ł. Piękoś, M. Andrzejak, M. P. Mitoraj, *Chem. Eur. J.* 2015, 21, 15299– 15307;

11e F. Sagan, M. P. Mitoraj, Non-covalent Interactions in Selected Transition Metal Complexes in Transition Metals in Coordination Environments, Springer 2019.

12

12a N. Mandal, S. M. Pratik, A. Datta, *J. Phys. Chem. B* 2017, 121, 825– 834;

12b A. Krapp, G. Frenking, E. Uggerud, *Chem. Eur. J.* 2008, 14, 4028– 4038.

13 J. Echeverría, G. Aullón, D. Danovich, S. Shaik, S. Alvarez, *Nat. Chem.* 2011, 3, 323– 330.

14 D. Danovich, S. Shaik, F. Neese, J. Echeverría, G. Aullón, S. Alvarez, *J. Chem. Theory Comput.* 2013, 9, 1977– 1991.

15

15a I. Cukrowski, F. Sagan, M. P. Mitoraj, *J. Comput. Chem.* 2016, 37, 2783– 2798;

15b C. F. Matta, S. A. Sadjadi, D. A. Braden, G. Frenking, *J. Comput. Chem.* 2016, 37, 143– 154;

15c F. Weinhold, P. R. Schleyer, W. C. McKee, *J. Comput. Chem.* 2014, 35, 1499– 1508;

15d J. Poater, M. Solà, F. M. Bickelhaupt, *Chem. Eur. J.* 2006, 12, 2889– 2895;

15e K. Eskandari, C. V. Alsenoy, *J. Comput. Chem.* 2014, 35(26), 1883– 1889;

15f R. W. F. Bader, *Chem. Eur. J.* 2006, 12(10), 2896– 2901;

15g J. Hernández-Trujillo, C. F. Matta, *Struct. Chem.* 2007, 18(6), 849– 857;

15h C. F. Matta, J. Hernández-Trujillo, T. H. Tang, R. F. W. Bader, *Chem. Eur. J.* 2003, 9, 1940– 1951;

15i P. L. A. Popelier, P. I. Maxwell, J. C. R. Thacker, I. Alkorta, *Theor. Chem. Acc.* 2019, 138: 12;

15j J. C. García-Ramos, F. Cortés-Guzmán, C. F. Matta, On the nature of hydrogen-hydrogen bonding, in Intermolecular interactions in crystals: fundamentals of crystal engineering, Royal Society of Chemistry, London 2018;

15k L. F. Pacios, L. Gómez, *Chem. Phys. Lett.* 2006, 432: 414– 420;

15l D. Myburgh, S. von Berg, J. Dillen, *J. Comput. Chem.* 2018, 39, 2273– 2282;

15m J. S. Lomas, *Magn. Reson. Chem.* 2019, 1– 15.

16 D. W. Szczepanik, *Comput. Theor. Chem.* 2016, 1080, 33– 37.

17 J. H. de Lange, I. Cukrowski, *J. Comput. Chem.* 2017, 38, 981– 997.

18 M. P. Mitoraj, A. Michalak, T. Ziegler, *J. Chem. Theory Comput.* 2009, 5, 962– 975.

19 R. Ponec, J. Roithová, *Theor. Chem. Acc.* 2001, 105, 383– 392.

20 R. F. W. Bader, Atoms in Molecules. A Quantum Theory, Oxford University Press, USA 1994.

21 M. A. Blanco, A. Martín Pendás, E. Francisco, *J. Chem. Theory Comput.* 2005, 1, 1096– 1109.

22 I. Cukrowski, *Comput. Theor. Chem.* 2015, 1066, 62– 75.

23

23a H. D. Rudolph, K. Walzer, I. Krutzik, *J. Mol. Spectrosc.* 1973, 47, 314– 339;

23b K. M. Gough, B. R. Henry, T. A. Wildman, *J. Mol. Struct.* 1985, 124, 71– 74;

23c R. Disselkamp, E. R. Bernstein, J. I. Seeman, H. V. Secor, *J. Chem. Phys.* 1992, 97, 8130– 8136;

23d A. Del Rio, A. Boucekkine, J. Meinnel, *J. Comput. Chem.* 2003, 24, 2093– 2100;

23eK. M. Gough, B. R. Henry, *J. Phys. Chem.* 1984, 88, 1298– 1302.

24 D. W. Szczepanik, M. Andrzejak, J. Dominikowska, B. Pawełek, T. M. Krygowski, H. Szatylowicz, M. Solà, *Phys. Chem. Chem. Phys.* 2017, 19, 28970– 28981.

25

25a J. Poater, R. Visser, M. Solà, F. M. Bickelhaupt, *J. Org. Chem.* 2007, 72, 1134– 1142;

25b J. Poater, M. Duran, M. Sola, *Front. Chem.* 2018, 6: 561.

26 Y. P. Yurenko, S. Bazzi, R. Marek J Kozelka, *Chem. Eur. J.* 2017, 23, 3246– 3250.

27

27a D. J. Wolstenholme, J. L. Dobson, G. S. McGrady, *Dalton Trans.* 2015, 44, 9718– 9731;

27b D. J. Wolstenholme, K. T. Traboulsee, Y. Hua, L. A. Calhoun, G. S. McGrady, *Chem. Commun.* 2012, 48, 2597– 2599;

27c D. J. Wolstenholme, E. J. Fradsham, G. S. McGrady, *CrystEngComm* 2015, 17, 7623– 7627.

28

28a C. Fonseca Guerra, T. van der Wijst, J. Poater, M. Swart, F. M. Bickelhaupt, *Theor. Chem. Acc.* 2010, 125, 245– 252;

28b O. A. Stasyuk, R. Sedlak, C. Fonseca Guerra, P. Hobza, *J. Chem. Theory Comput.* 2018, 14, 3440– 3450.

29 R. Firouzi, S. Shahbazian, *Struct. Chem.* 2014, 25, 1297– 1304.

30 J. Jara-Cortés, J. Hernández-Trujillo, *J. Comput. Chem.* 2018, 39, 1103– 1111.

31 M. G. Babashkina, D. A. Safin, M. P. Mitoraj, F. Sagan, M. Bolte, A. Klein, *Cryst. Growth Des.* 2016, 16, 3287– 3296.

32 N. K. V. Monteiro C L Firme, *J. Phys. Chem. A* 2014, 118, 1730– 1740.

33 H. A. Al-Ghulikah, A. Gopalan, L. P. S. Vahisan, M. A. Khalaf, H. A. Ghabbour, A. A. El-Emam, M. J. Percino, S. Thamotharan, *J. Mol. Struct.* 2020, 1199: 127019.